ANTIOXIDANTS & REDOX SIGNALING
Volume 6, Number 1, 2004

Forum Original Research Communication

Potential Role for Antiangiogenic Proteins in the Evolution of Bronchopulmonary Dysplasia

MARIA LYN QUINTOS-ALAGHEBAND,[1,3] CARL W. WHITE,[2] and MARGARET A. SCHWARZ[1,4]

ABSTRACT

Impaired neovascularization is associated with the pathologic presentation of bronchopulmonary dysplasia (BPD). To determine if neovascularization and factors that negatively influence blood vessel formation play a role in the evolution of BPD, we examined the temporospatial distribution of a protein known to inhibit fetal lung neovascularization with associated dysplastic lung formation, endothelial-monocyte activating polypeptide (EMAP) II. Immunohistochemical analysis of EMAP II in lung tissues of human infants with BPD indicated an elevation in EMAP II abundance as compared with control. Utilizing a baboon model, western analysis indicated that EMAP II was increased twofold in those baboons with pathologic signs of BPD as compared with gestational controls. Consistent with our findings in human tissues, immunohistochemistry and *in situ* hybridization demonstrate that EMAP II is highly expressed in the perivascular stroma and dysplastic lung periphery in neonatal baboons with BPD as compared with controls. Lastly, there is a premature acceleration in EMAP II's perivascular distribution in term newborn baboon as compared with gestational control. The marked increase in EMAP II's temporal expression, its distribution in the perivascular and dysplastic alveolar regions of the lungs, and the interruption in vasculogenesis in BPD suggest that neovascularization and factors that negatively influence blood vessel formation may play a role in BPD evolution. *Antioxid. Redox Signal.* 6, 137–145.

INTRODUCTION

BRONCHOPULMONARY DYSPLASIA (BPD) is a complex, multifaceted, and poorly understood disease process that was first described by Northway *et al.* in 1967 (11). BPD is defined by the clinical spectrum of a disease characterized by significant respiratory problems, a requirement for supplemental oxygen persisting beyond 1 month of age, and mechanical ventilation in the newborn period. The pathologic lesions in the human infant with BPD reflect the underdeveloped state of the lung that is thought to be related to the extensive injury, repair, and remodeling that occur in the postnatal period (5). This suggests that preterm infants develop BPD in response to the vulnerabilities of the later stages of lung development.

Although the hallmark of microscopic examination of the lungs in BPD is marked pulmonary hypoplasia, recent evidence indicates that there is a notable dysmorphic vascular pattern (3). In particular, infants with BPD exhibit two distinct findings: (a) pathologic changes in the lung periphery and (b) an interruption in the vascularization process (3). The combined manifestation of hypoplasia and dysmorphic vasculature suggests a possible link between morphogenesis and neovascularization during the later stages of lung development.

[1]Department of Critical Care and Cardiothoracic Surgery, Children's Hospital of Los Angeles USC–Keck School of Medicine, Los Angeles, CA 90027.
[2]Department of Pediatrics, National Jewish Medical and Research Centers, Denver, CO 80206.
[3]Currently at Winthrop University Hospital, Department of Pediatrics, Mineola, NY 11501.
[4]Currently at UMDNJ–Robert Wood Johnson Medical School, Departments of Surgery and Pediatrics, New Brunswick, NJ 08903.

This is supported by recent reports indicating that disruption of vascular formation leads to gross abnormalities of lung morphology (8, 17, 19, 21). Thus, we hypothesized that the inhibition of vascular development in premature infants may contribute to the cellular loss, inhibition of lung morphogenesis, and the subsequent dysplasia found in infants with BPD.

To explore the relationship between the vasculature and the formation of BPD, our objective was to examine the distribution of an antiangiogenic protein shown to have a role in lung development, endothelial-monocyte activating polypeptide (EMAP) II, in an established model of BPD. We chose EMAP II because: (a) EMAP II mRNA and protein are highly expressed during the pseudoglandular stage in which there is less pulmonary vascular development; (b) EMAP II localizes to the epithelial–mesenchymal junction prior to its marked down-regulation on entering the canalicular stage; (c) delivery of exogenous mEMAP II in a fetal lung allograft model markedly decreased lung neovascularization, induced lung dysplasia, and inhibited differentiation; and (d) delivery of an EMAP II blocking antibody enhanced neovascularization and accelerated differentiation of the lung periphery (17).

In a baboon model of BPD, we found the following: (a) a twofold increase in EMAP II protein concentration in baboon infants with BPD as compared with gestational controls; (b) a marked increase in EMAP II mRNA and protein products localizing to the perivascular and dysplastic alveolar or peripheral regions of lungs of animals with BPD; and (c) a premature acceleration in EMAP II's distribution to the perivascular regions comparable to EMAP II expression in a term infant. Similar results were found in lung tissue obtained from human neonates that had BPD. Thus, our data suggest that the untimely increase in EMAP II and acceleration in its expression in perivascular regions may have a role in the pathogenesis of lung dysplasia in BPD. Furthermore, these findings suggest a link between lung hypoplasia, failure of neovascularization, and antiangiogenic proteins in the evolution of BPD.

MATERIALS AND METHODS

Western blot analysis

Frozen fetal baboon lung tissues were obtained from the Program for Collaborative Research on BPD, based at the Southwest Foundation for Biomedical Research, San Antonio, Texas (4). Distal left lower lobe lung sections were secured from the later stages of baboon lung development. Specifically, lungs were acquired from control animals on days 125 (late canalicular stage), 140 (saccular stage), 160, and 175 (normal gestation = 186 days). Lungs were also obtained on prematurely born baboons that developed BPD at 125 days of gestation plus 6 days, 14 days, and 21 days of oxygen delivery (125d + 6d, 125d + 14d, and 125d + 21d, respectively) (n = 4–8 animals per group, performed on two different occasions). Left lower lobe lung sections were snap-frozen and stored at −70°C. Lungs were then homogenized by sonification in 50 m*M* Tris, pH 7.4, 0.9 *M* NaCl, 0.01% NaN_3, and protease inhibitors with a Branson sonifier. Homogenates were cleared by centrifugation at 14,000 rpm for 20 min, the protein concentration determined by Bradford analysis (Bio-Rad, Hercules, CA, U.S.A.), and the samples normalized by protein content. Equal amounts of protein were subjected to electrophoresis on a 12% sodium dodecyl sulfate–polyacrylamide gel electrophoresis gel, transferred to Immobilon-P, blocked overnight in a casein-based blocking solution (Boehringer Mannheim, Indianapolis, IN, U.S.A.), and probed with a rabbit anti-EMAP II antibody (polyclonal monospecific antibody based on immunoblotting of plasma and cell extracts). Specific binding was detected with chemiluminescence substrate (Pierce, Rockford, IL, U.S.A.) and XAR-5 film (Eastman Kodak, Rochester, NY, U.S.A.). Quantitative analysis was accomplished using NIH Image, and samples were normalized for background.

Immunohistochemistry

Immunohistochemistry of paraffin-embedded sections of fetal lung were obtained from two sources. Baboon lung was obtained from the baboon breeding colony at the Southwest Foundation for Biomedical Research facility. Proximal and distal sections were secured from the later stages of baboon lung development. Specifically, lungs were acquired from control animals on days 125 (late canalicular stage), 140 (saccular stage), 160, and 175 (normal gestation = 186 days). Lungs were also obtained on prematurely born baboons that developed BPD at 125d + 14d (n = 3 animals per time point). Archival proximal and distal lung tissue from infant lungs was obtained following approval of the Committee on Clinical Investigations at Children's Hospital of Los Angeles. Tissue was obtained from routine autopsies performed on infants that had developed BPD without other complicating factors (n = 4) and compared with lung tissue obtained from gestational controls that had no history of lung disease (n = 3) (see Table 1). Human specimens were formalin-fixed and paraffin-embedded as per pathology department's routine protocol. Age-matched controls were chosen based on their full-term status, having no defined lung pathology at the time of demise, and their postgestational age approximating that of children with BPD. Paraffin-embedded lung sections from both human infants and the baboon model of BPD were deparaffinized and underwent peroxide quenching. Utilizing a histostain kit from Zymed (San Francisco, CA, U.S.A.), sections were blocked, exposed to anti-EMAP II IgG (5 μg/ml) (17) overnight at 4°C, and then incubated with secondary biotinylated antibody according to the manufacturer's protocol. A brief incubation with the streptavidin–horseradish peroxidase conjugate system was followed by development with the chromogen substrate 3-amino-9-ethylcarbazole. BPD subject samples were processed simultaneously with controls. The chromogenic substrate step was stopped at exactly the same time in the subjects with BPD as the controls. Lung sections were evaluated using light microscopy.

In situ hybridization

Representative samples of baboon lung from gestational controls and from animals exposed to PRN (pro re nata, or as occasion requires) oxygen (BPD model) were used for *in situ* hybridization. *In situ* hybridization of paraffin-embedded sections of distal and proximal fetal lung were obtained from baboons during the later stages of baboon lung development (days

TABLE 1. PROFILE OF STUDY POPULATION

BPD subjects		*Control*	
11 days old 26–27 weeks AOG BW 960 g	BPD severe Gr I–II art. PHTN	7 days old	Normal lungs Hydrocephalus
3 months old 32 weeks AOG BW 2,320 g	BPD Reparative stage	2 months old	Normal lungs SIDS
4 weeks old 22 weeks AOG BW 520 g	BPD severe PDA	1 year old	Normal lungs Leukoencephalopathy
5 weeks old 25 weeks AOG BW 748 g	BPD severe Pseudomonas sepsis		

AOG, age of gestation; BW, body weight; PDA, patent ductus arteriosus; PHTN, pulmonary hypertension; SIDS, sudden infant death syndrome.

125–175 with normal gestation = 186 days) and from baboons that developed BPD to determine the normal spatial distribution of EMAP II ($n = 3$ animals per time point). As previously described (20), digoxigenin (Dig) RNA probe antisense and sense (control) were made with the DigRNA labeling kit (SP6/T7) from Boehringer Mannheim. Lungs were fixed in 4% paraformaldehyde in diethyl pyrocarbonate (DEPC)-treated water, dehydrated with ethanol, and then embedded in paraffin. Using DEPC-treated equipment and solutions, we sectioned the paraffin-embedded specimens, and they were rehydrated and incubated in a prewarmed proteinase K (Sigma, St. Louis, MO, U.S.A.) solution (5 μg/ml). Slides were then reimmersed in 4% paraformaldehyde, treated with 0.25% acetic anhydride, and dehydrated. Sections were exposed to a hybridization solution containing 50% formamide, 10% dextran sulfate, 1 mg/ml tRNA, 1× Denhardt's solution, 4× saline–sodium citrate (SSC), 50 m*M* Tris, and 5 m*M* EDTA that contained 150–300 ng/ml Dig-labeled RNA probe at 50°C overnight. The RNA probe for EMAP II was 456 bp in size and obtained from a region that has a minimal homology with other known proteins. The slides were washed at 55°C in 2× SSC 50% formamide, 1× SSC, and 0.1× SSC for 30 min before being incubated with RNase A (20 μg/ml) for 30 min at 37°C. Slides were then rinsed with 2× SSC, and Dig nucleic acid detection was accomplished with the Genius 3 kit from Boehringer Mannheim. In brief, slides were incubated in 0.1 *M* maleic acid 0.15 *M* NaCl, pH 7.5, for 5 min, and then they underwent blocking in a 1% block reagent. After the blocking, the slides were incubated with anti-Dig-alkaline phosphatase conjugate at 4°C overnight. Slides were then rinsed and incubated with a dilute 5-bromo-1-chloro-3-indoyl phosphate/nitro blue tetrazolium solution for 3 h at room temperature. Development of control and BPD slides was performed simultaneously with all slides having equal exposure times. Afterward, slides were counterstained with a 0.02% fast green solution for 2 min, rinsed in water, air-dried, and mounted. The entire lung section was analyzed using light microscopy for distribution and intensity of EMAP II transcripts.

Statistics

Statistical analysis was performed using a nonpaired Student's *t* test, one-way ANOVA, followed by Student–Newman–Keuls and Mann–Whitney analysis on the computer program Statview.

RESULTS

Spatial expression of EMAP II in a baboon model with BPD

In situ hybridization and immunohistochemistry of paraffin-embedded sections of fetal lung during the later stages of baboon lung development were used to determine the normal spatial distribution of EMAP II. Results were compared with those tissues of newborn baboons that developed BPD following premature delivery and exposure to 14 days of PRN oxygen therapy. *In situ* hybridization in developing baboon lungs revealed a gradual decrease in EMAP II expression in the alveolar regions during late gestation. During the canalicular stage, 125 days (Fig. 1A), EMAP II mRNA was expressed diffusely throughout the subepithelial region of the bronchi (white arrows) and the alveolar septal regions (filled arrows), whereas EMAP II mRNA expression in the perivascular region was minimal (open arrow). By the beginning of the saccular stage, 140 days (Fig. 1B), there was a slight increase in its perivascular expression (open arrow) and a decrease in distal alveolar expression (filled arrows). Near term, 160 days and 175 days (Fig. 1C and D, respectively), EMAP II mRNA expression was predominately concentrated in the perivascular regions. In contrast, *in situ* hybridization in baboons with BPD, at 125 days of gestation plus 14 days of oxygen exposure (Fig. 2B), revealed that EMAP II mRNA was concentrated in the perivascular and peribronchial region similar to that seen in the later gestational age of 175 days (Fig. 1D) with a notable decline in its distal alveolar expression. In contrast, 140-

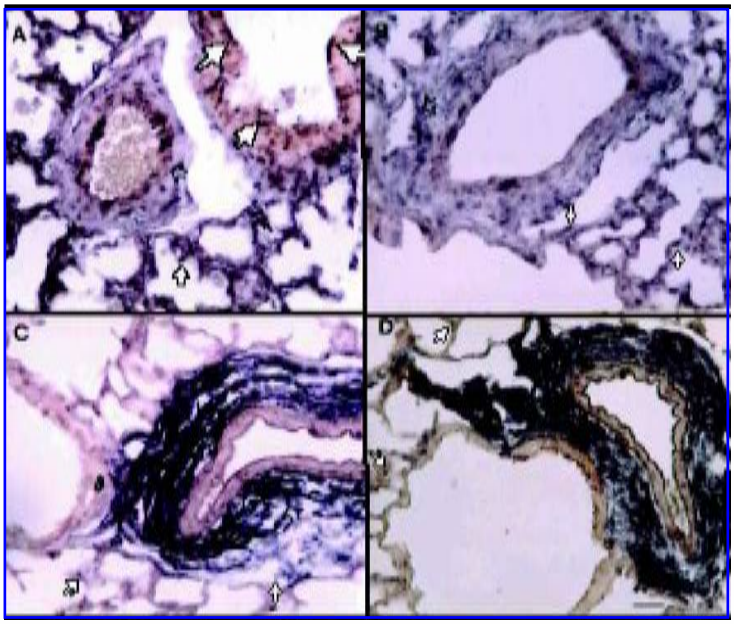

FIG. 1. ***In situ*** **hybridization in baboon tissue indicates that EMAP II mRNA at 125 days (canalicular stage) is expressed throughout the subepithelium of the bronchi (white arrows, A) and diffusely in the distal alveolar regions (filled arrows, A), whereas EMAP II mRNA expression in the perivascular region is minimal (open arrow, A).** By the beginning of the saccular stage, 140 days (**B**), there is a slight increase in its perivascular expression, but a decrease in its overall lung expression (filled arrows, B). Near term, 160 days and 175 days (**C** and **D**, respectively), EMAP II mRNA expression is predominately limited to the stroma in the perivascular region with minimal alveolar expression (filled arrows, C and D). Bar = 250 μm in A–D.

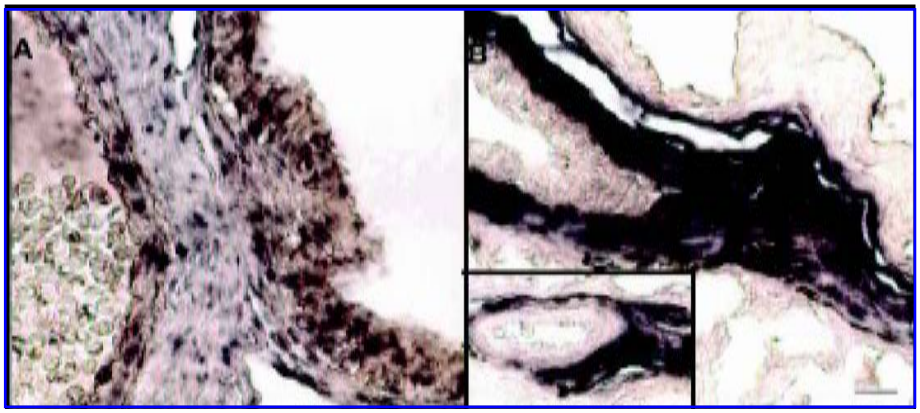

FIG. 2. ***In situ*** **hybridization indicates that EMAP II mRNA expression is markedly increased in baboons with BPD lung following early delivery at 125 days of gestation followed by exposure to 14 days of oxygen therapy (B).** The increased expression and distribution of EMAP II mRNA in baboons (B) with BPD are similar to those seen in the later gestational age of 175 days (Fig. 1D), where there is a marked increase in the expression of EMAP II mRNA in the peribronchial (B) and perivascular stroma (inset, B) with a notable decline in distal alveolar expression. This is in direct contrast to the 140-day gestational control animal (**A** and Fig. 1B), where there is only minimal perivascular stromal and subepithelial bronchial expression. Bar = 500 μm in A and B.

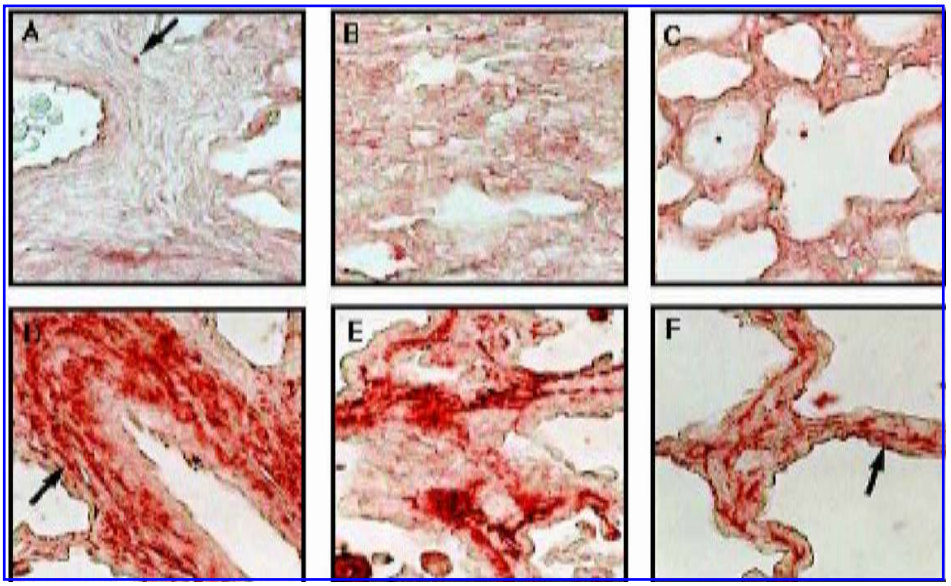

FIG. 3. Immunohistochemistry indicates that EMAP II abundance is markedly increased in the proximal, transitional epithelial zone, and distal alveolar region of those baboons with BPD. Baboon infants from 125 days of gestation plus 14 days of oxygen delivery, with pathologic signs of BPD, have an increased and intense expression of EMAP II surrounding the vessels (**D**; arrow indicates perivascular region), the transitional bronchial epithelium to distal alveolar zone (**E**), and the distal alveolar regions (**F**; arrow indicates EMAP II expression in the distal alveolar region) of the lungs. In contrast, the 140 day gestational control indicates that EMAP II is minimally expressed in the perivascular stroma and distal alveolar regions of the lung (**A:** arrow indicates expression in the vessel region; **B:** transitional bronchial epithelium to distal alveolar zone; **C:** distal alveolar regions). Magnification is ×400 in A–F.

day gestational control animals (Figs. 2A and 1B) showed minimal perivascular and peribronchial expression and low levels of distal alveolar expression. Immunolocalization of EMAP II protein verifies our *in situ* hybridization findings. EMAP II spatial expression in baboons with BPD (125d + 14d) was markedly increased in the perivascular region (Fig. 3D), the transitional bronchial epithelium to distal alveolar zone (Fig. 3E), and the distal alveolar region (Fig. 3F) as compared with similar regions in the 140-day gestational control animal (Fig. 3A–C).

Temporal expression of EMAP II protein in baboon lung model of BPD

EMAP II expression was increased in the lungs of baboons with BPD. Equal amounts of lung protein extracts from 125-, 140-, 160-, and 175-day fetal lungs were subjected to western analysis (n = 4–8 animals per group, performed on two different occasions). These studies indicated that EMAP II expression decreases between days 125 (late canalicular stage) and 140 (early saccular stage). Thereafter, it remains low until just prior to term at day 175 (Fig. 4A). In contrast to its normal decline between days 125 and 160, EMAP II protein abundance was markedly elevated in animals with BPD (125d + 6d, 125d + 14d, and 125d + 21d) as compared with its diminished levels in the 140-day gestational controls ($p < 0.05$). In fact, EMAP II abundance in the BPD animal was similar to that expressed by those animals just prior to term delivery at 175 days (Fig. 4B) (n = 4–8 animals per group, performed on two different occasions) in lungs of these 125-day gestation premature baboons.

Spatial expression of EMAP II protein in human tissue with BPD compared with age-matched controls

Analysis of EMAP II protein distribution in human tissue was performed on paraffin-embedded lung tissue sections from autopsies of four neonates with a clinical diagnosis and histopathologic findings consistent with BPD. These results were compared with three age-matched control patients with histopathologically normal lungs (Table 1). All sections were subjected to immunohistochemistry for EMAP II. Consistent with our findings in the neonatal baboon with BPD, immunolocalization of EMAP II in lung tissue of the human neonate with pathologic signs of BPD showed a marked increase in EMAP II expression in perivascular regions (Fig. 5B, arrows) (n = 4 subjects with four lung samples analyzed per patient on two different occasions) as compared with age-matched control (Fig. 5A, arrows) (n = 3 subjects with four lung samples analyzed per patient on two different occasions). In addition, similar to findings in the baboon, there was a marked diffuse increase in EMAP II expression throughout the peripheral

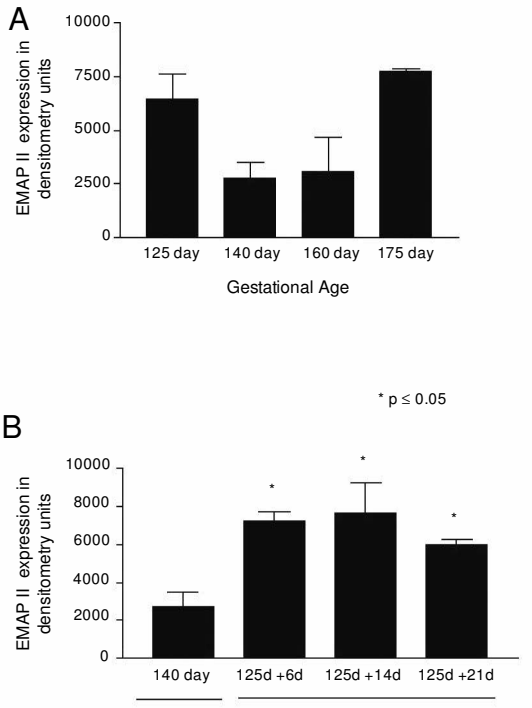

FIG. 4. Western analysis revealed a marked increase in EMAP II protein in those animals with BPD as compared with gestational controls. Analysis of equal amounts of lung protein extracts from gestational animals (normalized for background and analyzed by NIH Image analysis) indicated that EMAP II expression decreased between days 125 and 140 (**A**). EMAP II expression remained low until just prior to term at day 175 (A). In contrast, EMAP II expression in those baboons that developed BPD (**B**) was elevated twofold ($*p < 0.05$), similar to levels expressed by those animals just prior to delivery at 175 days, as compared with gestational control of 140 days (**B**). n = 4–8 animals per group performed on two different occasions. Analysis was performed using ANOVA followed by Student–Newman–Keuls and Mann–Whitney.

lung in infants with BPD (Fig. 6B, arrows in inset) as compared with controls (Fig. 6A). This result was consistent in all human lungs with BPD versus our control population.

DISCUSSION

Herein, we describe a marked increase in the mRNA and protein concentration of the antiangiogenic protein EMAP II in BPD, both in the human disorder and in the baboon model, as compared with normal or control lungs. EMAP II appeared at an accelerated rate within the perivascular region and was widely expressed throughout the dysplastic peripheral lung in those neonates with BPD. This abnormal increase in EMAP II during this critical stage of lung proliferation and morphogenesis suggests that altered vascularization, and in particular antiangiogenic proteins, may play a role in the pathogenesis of this complex disorder.

BPD remains a major cause of morbidity in premature infants (1). Since its original description, several efforts were made to define its cause. There are four key elements in BPD pathogenesis: (a) host susceptibility (prematurity, fetal asphyxia), (b) primary lung injury (structural and biochemical immaturity, surfactant deficiency), (c) secondary lung injury (surfactant dysfunction, barotrauma, oxygen toxicity, and inflammatory mediators), and (d) abnormal lung repair (fibrosis) (14). Histological studies in BPD have revealed alternating regions of fibrosis and hyperinflation. BPD is characterized by marked alveolar hypoplasia, fibrosis, and a dysmorphic vascular pattern. Specifically, a marked reduction in lung capillaries and small vessels has been noted. Although most investigators agree that the four key elements mentioned play a role in BPD evolution, the cell biologic basis for interactions between these factors remains poorly understood.

Morphometric analysis of lungs of primates with BPD reveals a reduction in median radial alveolar counts and lung internal surface area consistent with impaired alveolar development (6). In addition, a secondary loss of arterial diameter contributes to a reduction in the volume of the vascular bed (13). One possible etiology for the impaired vessel formation is the presence of lower levels of the endothelial mitogen vascular endothelial growth factor (VEGF) found in airway fluid samples from premature infants during development of BPD as compared with those surviving without BPD (9). This observed decrease in VEGF expression is similar to that seen in a neonatal rabbit lung hyperoxia injury model. Maniscalco *et al.* (10) observed a marked decrease in lung alveolar VEGF mRNA and protein levels in rabbits exposed to 9 days of hyperoxia. These findings suggest that decreased VEGF expression contributes to the impaired postnatal microvascular development due to oxygen injury.

The exact mechanisms regulating pulmonary vascular development are incompletely defined. However, normal neonatal lung growth requires a substantial increase in microvascular endothelial cells. This period of rapid vascularization starts during the third stage of normal lung development known as the canalicular stage. The canalicular stage extends from 16 to 28 weeks of gestation in the human and, although less clearly defined in the baboon, 125 days of gestation is within the canalicular stage. The canalicular stage brings about important changes in lung structure with important functional significance. The multiplication of capillaries and the differentiation of type I to type II pneumocytes give the lung the capability to synthesize surfactant and lead to the establishment of an air/blood interface that allows efficient gas exchange. Any disturbance in lung neovascularization or an imbalance between the factors that govern it adversely affects the transition to mature lung structure. Furthermore, recent data suggest that the same pattern of regulation is evident during neovascularization. Flk-1 positive cells exposed to VEGF from the surrounding mesenchyme become endothelial cells. By contrast, exposure to platelet-derived growth factor-BB (PDGF-BB) from the mesenchyme will redirect these cells to become smooth muscle cells or pericytes (2, 18). Knowledge of down-regulation of VEGF with hyperoxia and in BPD, coupled with the findings that precursor endothelial cells can be redirected to become smooth muscle cells if VEGF levels are low, suggests that the growth factor and cytokine milieu markedly influences the lung's ability to form a normal vasculature during the critical canalicular (vascular) stage.

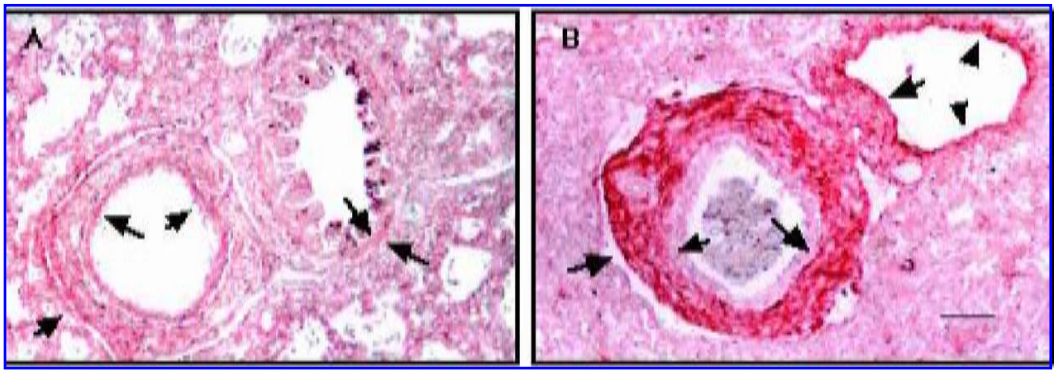

FIG. 5. Immunolocalization of EMAP II perivascular expression in the human neonate with BPD is consistent with that seen in those baboons with BPD. Examination of human neonatal lungs that exhibited pathologic signs of BPD indicated that EMAP II expression is markedly increased in the perivascular region (as indicated by the arrows in **B**). This is depicted by a typical central region of the lung obtained from the 11-day-old infant with severe BPD indicated as the first infant in Table 1. In contrast, age-matched control infants had minimal expression of EMAP II in the perivascular region (**A**; arrows indicate vessels) as indicated by a characteristic central region obtained in a 7-day-old child with hydrocephalus (second infant in Table 1). Bar = 250 μm in A and B.

A direct link between lung morphogenesis and altered neovascularization is indicated by our understanding of vascular formation. The vasculature is formed by two predominant forces during development, vasculogenesis and angiogenesis (7, 12), with neovascularization being dependent on epithelial–mesenchymal interactions to guide vessel formation. Vasculogenesis is involved in the formation of the first primitive vasculature and is mediated by the transdifferentiation of mesodermal cells into endothelial cells that then organize and condense into vascular structures. In contrast, angiogenesis is characterized by the extension of previously formed vessels into undervascularized regions. The importance of normal

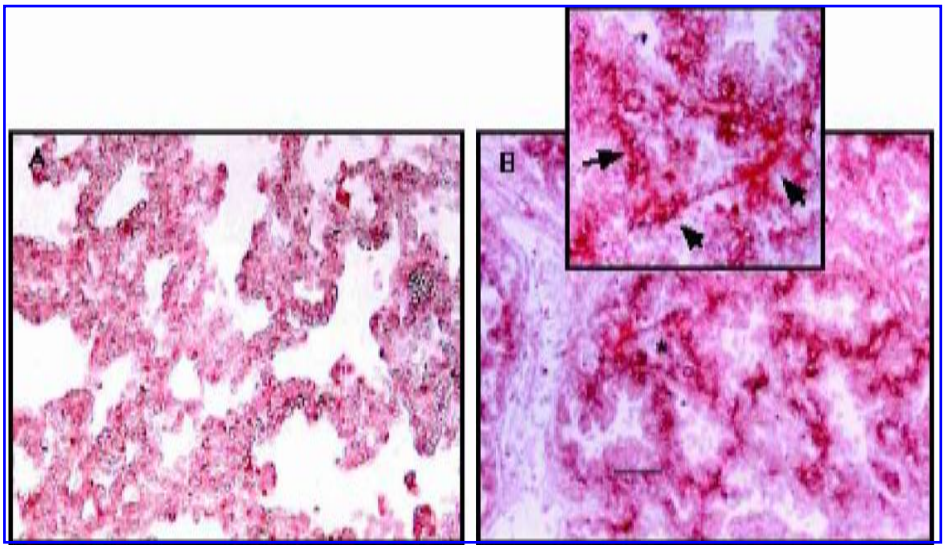

FIG. 6. EMAP II immunohistochemical expression in the human neonate with BPD is markedly increased in the distal alveolar region consistent with those baboons with BPD. Tissue obtained from human neonates with pathologic signs of BPD (**B**; inset is of the region indicated by the asterisk, and the arrows indicate EMAP II expression in the distal alveolar region) had a marked diffuse increase in EMAP II expression in the alveolar region. This representative region comes from a 5-week-old child with severe BPD listed as the fourth child in Table 1. In contrast, age-matched control infants (**A**) had minimal expression of EMAP II in this region. This classic region was taken from the distal areas of a 1-year-old control with leukoencephalopathy listed in Table 1. Bar = 250 μm in A and B, 500 μm in B inset.

progression of lung neovascularization and normal morphologic development is supported by studies in which: (a) mice overexpressing VEGF transgene using a lung-specific surfactant protein-C promoter demonstrate marked increase in lung vasculature, disrupted branching morphogenesis, and inhibition of type I cell differentiation (19); (b) lung-specific inhibition of the structural maturation gene transforming growth factor β1 results in mice with vascular malformations and an arrest of lung sacculation and epithelial cell differentiation (21); and (c) excess amounts of the antiangiogenic protein EMAP II in fetal lung allografts result in a decrease in vessel density, an arrest in distal lung epithelial differentiation resulting in cellular loss, reduction in surfactant protein-C expression, and markedly dysplastic alveolar epithelial cells (17). These and other studies indicate that there is a direct relationship between lung neovascularization and normal lung morphologic development.

After a role for neovascularization and EMAP II in the finely regulated process of lung morphologic development had been established, it was a natural extension of our work to examine a pathologic process that had dysmorphic vascular formation, BPD. The baboon BPD model is a well defined, reliable, and controlled model that allows us to make observations on well perserved tissue. The normal perivascular distribution [as defined by colocalization of EMAP II and platelet-endothelial cell adhesion molecule-1 (PECAM-1)] and decreased EMAP II mRNA and protein during the canalicular stage of baboon fetal lung development are consistent with our findings in murine lung development (15). In contrast, in the baboon model of BPD, lung EMAP II protein expression is elevated twofold above gestational control. This increase in EMAP II abundance during this critical stage of vascular development may contribute to an interruption in blood vessel formation and subsequently impact distal airway epithelial morphogenesis. This hypothesis is supported by our previous findings that delivery of exogenous mEMAP II in a fetal lung allograft model markedly decreased lung neovascularization, induced lung dysplasia, and inhibited distal alveolar differentiation (17), thus suggesting that the premature elevation of EMAP II may contribute to the classic disease pattern of microvascular and alveolar hypoplasia characteristic of BPD. Furthermore, what was equally interesting was that EMAP II mRNA and protein expression during this critical stage was accelerated in its abundance and distribution, resembling the lung of a near-term infant. This accelerated expression and distribution of EMAP II suggest that EMAP II may be prematurely exerting a negative influence on vascular development. Alternatively, the abnormal persistence of alveolar EMAP II could equally effectively inhibit distal vessel formation. Based on our previous findings, we hypothesize that the vessel disruption may be due in part to EMAP II's ability to induce targeted apoptosis in the migrating and dividing endothelial cells (16). Together, these findings suggest that abnormal EMAP II distribution and expression could contribute to the subsequent disruption of neovascularization and ultimately lung morphologic development.

In summary, we have demonstrated that there is a marked increase in the temporal expression of the antiangiogenic protein EMAP II in BPD. EMAP II's spatial expression and distribution are altered such that they are comparable to that of a term infant. Thus, its localization is predominately in the perivascular stroma and dysplastic lung periphery. EMAP II's change in expression and distribution is consistent with that of a modulator that may have a significant influence on BPD lung pathology. Furthermore, these findings are consistent with the hypothesis that premature disruption of lung neovascularization may play an important role in the pathogenesis of BPD. Lastly, this study suggests that antiangiogenic proteins, such as EMAP II, may have a role in BPD pathogenesis. We speculate that premature birth exposes the neonatal lungs to factors that negatively influence neovascularization. This exposure then directly or indirectly results in the up-regulation of those factors that negatively affect neovascularization. These speculations are the basis of our ongoing research.

AKNOWLEDGMENTS

We would like to give special thanks to Jie Lui and Fongrang Zhang for their excellent technical skills. The authors acknowledge the superb and dedicated assistance of numerous scientists, physicians–scientists, nurses, respiratory therapists, and other personnel at the BPD Resource Center in San Antonio, Texas, supported by NIH HL-52636. Research was supported in part by the American Lung Association RG-084-N (M.A.S.), CI-001N (M.A.S.), the Webb–Berger Foundation (M.A.S.), NIH HL-60061 (M.A.S.), NIH HL-03981 (M.A.S.), and NIH HL-56263 (C.W.W.).

ABBREVIATIONS

BPD, bronchopulmonary dysplasia; DEPC, diethyl pyrocarbonate; Dig, digoxigenin; EMAP II, endothelial-monocyte activating polypeptide II; PRN, pro re nata (as occasion requires); SSC, saline–sodium citrate; VEGF, vascular endothelial growth factor.

REFERENCES

1. Avery, ME, Tooley WH, Keller JB, Hurd SS, Bryan MH, Cotton RB, Epstein MF, Fitzhardinge PM, Hansen CB, Hansen TN, *et al.* Is chronic lung disease in low birth weight infants preventable? A survey of eight centers. *Pediatrics* 79: 26–30, 1987.
2. Carmeliet P. Developmental biology. One cell, two fates. *Nature* 408: 43, 45, 2000.
3. Coalson JJ. Experimental models of bronchopulmonary dysplasia. *Biol Neonate* 1: 35–38, 1997.
4. Coalson JJ, Kuehl TJ, Escobedo MB, Hilliard JL, Smith F, Meredith K, Null D Jr, Walsh W, Johnson D, and Robotham JL. A baboon model of bronchopulmonary dysplasia. II. Pathologic features. *Exp Mol Pathol* 37: 335–350, 1982.
5. Coalson JJ, King RJ, Yang F, Winter V, Whitsett JA, Delemos RA, and Seidner SR. SP-A deficiency in primate model of bronchopulmonary dysplasia with infection. In situ mRNA and immunostains. *Am J Respir Crit Care Med* 151: 854–866, 1995.

6. Coalson JJ, Winter V, and deLemos RA. Decreased alveolarization in baboon survivors with bronchopulmonary dysplasia. *Am J Respir Crit Care Med* 152: 640–646, 1995.
7. Coffin JD, Harrison J, Schwartz S, and Heimark R. Angioblast differentiation and morphogenesis of the vascular endothelium in the mouse embryo. *Dev Biol* 148: 51–62, 1991.
8. Jakkula M, Cras T, and Abman S. Effects of fumagillin and thalidomide treatment on alveolarization in the developing rat lung. *Pediatr Res* 45: 67A, 1999.
9. Lassus P, Ristimaki A, Ylikorkala O, Viinikka L, and Andersson S. Vascular endothelial growth factor in human preterm lung. *Am J Respir Crit Care Med* 159: 1429–1433, 1999.
10. Maniscalco WM, Watkins RH, D'Angio CT, and Ryan RM. Hyperoxic injury decreases alveolar epithelial cell expression of vascular endothelial growth factor (VEGF) in neonatal rabbit lung. *Am J Respir Cell Mol Biol* 16: 557–567, 1997.
11. Northway W Jr, Rosan RC, and Porter DY. Pulmonary disease following respirator therapy of hyaline-membrane disease. Bronchopulmonary dysplasia. *N Engl J Med* 276: 357–368, 1967.
12. Poole TJ and Coffin JD. Vasculogenesis and angiogenesis: two distinct morphogenetic mechanisms establish embryonic vascular pattern. *J Exp Zool* 251: 224–231, 1989.
13. Reid L. Bronchopulmonary dysplasia—pathology. *J Pediatr* 95: 836–841, 1979.
14. Rogers M, Nichols D, Mellema J, and Martin L. Chronic lung disease in infants and children. In: *Textbook of Pediatric Intensive Care*, 3rd edit., edited by Rogers M. Baltimore: Williams and Wilkins, 1996, pp. 166–174.
15. Schwarz M, Lee M, Zhang F, Zhao J, Jin Y, Smith S, Bhuva J, Stern D, Warburton D, and Starnes V. EMAP II: a modulator of neovascularization in the developing lung. *Am J Physiol* 276: L365–L375, 1999.
16. Schwarz MA, Kandel J, Brett J, Li J, Hayward J, Schwarz RE, Chappey O, Wautier JL, Chabot J, Lo Gerfo P, and Stern D. Endothelial-monocyte activating polypeptide II, a novel antitumor cytokine that suppresses primary and metastatic tumor growth, and induces apoptosis in growing endothelial cells. *J Exp Med* 200: 341–353, 1999.
17. Schwarz MA, Zhang F, Gebb S, Starnes V, and Warburton D. EMAP II inhibits lung neovascularization and airway epithelial morphogenesis. *Mech Dev* 95: 123–132, 2000.
18. Yamashita J, Itoh H, Hirashima M, Ogawa M, Nishikawa S, Yurugi T, Naito M, and Nakao K. Flk1-positive cells derived from embryonic stem cells serve as vascular progenitors. *Nature* 408: 92–96, 2000.
19. Zeng X, Wert SE, Federici R, Peters KG, and Whitsett JA. VEGF enhances pulmonary vasculogenesis and disrupts lung morphogenesis in vivo. *Dev Dyn* 211: 215–227, 1998.
20. Zhang F and Schwarz MA. Temporo-spatial distribution of endothelial-monocyte activating polypeptide II, an anti-angiogenic protein, in the mouse embryo. *Dev Dyn* 218: 490–498, 2000.
21. Zhou L, Dey CR, Wert SE, and Whitsett JA. Arrested lung morphogenesis in transgenic mice bearing an SP-C-TGF-beta 1 chimeric gene. *Dev Biol* 175: 227–238, 1996.

Address reprint requests to:
Margaret A. Schwarz, M.D.
UMDNJ–Robert Wood Johnson Medical School
125 Paterson Street, CAB 7036
New Brunswick, NJ 08903

E-mail: m.schwarz@umdnj.edu

Received for publication September 24, 2003; accepted October 20, 2003.

This article has been cited by:

1. Rajesh S. Alphonse , Saima Rajabali , Bernard Thébaud . 2012. Lung Injury in Preterm Neonates: The Role and Therapeutic Potential of Stem Cells. *Antioxidants & Redox Signaling* **17**:7, 1013-1040. [Abstract] [Full Text HTML] [Full Text PDF] [Full Text PDF with Links]
2. Yao Chen, Susan K Legan, Anne Mahan, Janet Thornton, Haiming Xu, Margaret A Schwarz. 2012. Endothelial Monocyte Activating Polypeptide II Disrupts Alveolar Epithelial Type II to Type I Cell Transdifferentiation. *Respiratory Research* **13**:1, 1. [CrossRef]
3. Matthias Clauss, Robert Voswinckel, Gangaraju Rajashekhar, Ninotchka L. Sigua, Heinz Fehrenbach, Natalia I. Rush, Kelly S. Schweitzer, Ali Ö. Yildirim, Krzysztof Kamocki, Amanda J. Fisher, Yuan Gu, Bilal Safadi, Sandeep Nikam, Walter C. Hubbard, Rubin M. Tuder, Homer L. Twigg, Robert G. Presson, Sanjay Sethi, Irina Petrache. 2011. Lung endothelial monocyte-activating protein 2 is a mediator of cigarette smoke–induced emphysema in mice. *Journal of Clinical Investigation* **121**:6, 2470-2479. [CrossRef]
4. Chang Won Choi. 2011. Alveolar Aspect of Bronchopulmonary Dysplasia. *Journal of the Korean Society of Neonatology* **18**:2, 165. [CrossRef]
5. Su Jin Cho. 2011. Vascular Aspects of Bronchopulmonary Dysplasia. *Journal of the Korean Society of Neonatology* **18**:2, 177. [CrossRef]
6. P CHESS, C DANGIO, G PRYHUBER, W MANISCALCO. 2006. Pathogenesis of Bronchopulmonary Dysplasia. *Seminars in Perinatology* **30**:4, 171-178. [CrossRef]
7. C DEFELICE, S PARRINI, A BARDUCCI, G CHITANO, G TONNI, G LATINI. 2006. Abnormal oral mucosal light reflectance in bronchopulmonary dysplasia. *Early Human Development* **82**:4, 273-278. [CrossRef]
8. Kumuda C. Das . 2005. Thioredoxin and Its Role in Premature Newborn Biology. *Antioxidants & Redox Signaling* **7**:11-12, 1740-1743. [Abstract] [Full Text PDF] [Full Text PDF with Links]
9. JACQUES BOURBON, OLIVIER BOUCHERAT, BERNADETTE CHAILLEY-HEU, CHRISTOPHE DELACOURT. 2005. Control Mechanisms of Lung Alveolar Development and Their Disorders in Bronchopulmonary Dysplasia. *Pediatric Research* **57**:5 Part 2, 38R-46R. [CrossRef]
10. Kumuda C. Das . 2004. Redox Control of Premature Birth and Newborn Biology. *Antioxidants & Redox Signaling* **6**:1, 105-107. [Citation] [Full Text PDF] [Full Text PDF with Links]